Available online at www.sciencedirect.com
SCIENCE DIRECT®
Pergamon
Acta Materialia 51 (2003) 2149–2159
Acta MATERIALIA
www.actamat-journals.com

Interaction of recrystallization and precipitation: The effect of Al_3Sc on the recrystallization behaviour of deformed aluminium

M.J. Jones *, F.J. Humphreys

Manchester Materials Science Centre, Grosvenor Street, Manchester, M1 7HS, UK

Received 3 September 2002; accepted 29 December 2002

Abstract

The kinetics and mechanisms of recrystallization in high purity binary Al-Sc alloys have been investigated. In an Al-0.25wt.%Sc alloy, precipitation always precedes recrystallization, which is severely inhibited. However, in an Al-0.12wt.%Sc alloy, precipitation is found to either precede, follow or occur concurrently with recrystallization, depending on the processing conditions, and the resultant complex microstructures are interpreted in terms of the interactions between precipitation and recrystallization. Coherent precipitates are found to coarsen and become semi-coherent during the passage of low-angle boundaries during recovery. The passage of high-angle boundaries through semi-coherent precipitates during recrystallization occurs by migration of the boundary through the particle, resulting in the precipitates maintaining semi-coherency with the new grain.

Keywords: Recrystallization; Precipitation; Strain Induced Boundary Migration (SIBM); Grain boundary faceting; Zener pinning

1. Introduction

There is strong academic and industrial interest in recrystallization, particularly in aluminium alloys, driven by the need to understand and control this complex phenomenon in order to optimise properties through the careful control of thermo-mechanical processing schedules. Most research on the recrystallization of two-phase aluminium alloys has been undertaken on material in which the second phase is present during deformation and in which subsequent annealing does not substantially alter the phase distribution. However, in precipitation-hardening alloys, the situation may arise in which the processes of recrystallization and precipitation occur concurrently. If recrystallization of a deformed supersaturated solid solution is not complete before the start of precipitation, then the material may exhibit complex behaviour due to the mutual interaction of recrystallization and precipitation [1,2]. Thus the presence of a deformed microstructure may affect the nature and kinetics

* Corresponding author. Nowat: Département M.M.F., Ecole Nationale Supérieure des Mines de Saint Etienne, 158, cours Fauriel, F-42023 Saint-Etienne, France. Tel.: +33-477-420002; fax: +33-477-426678.
E-mail address: jones@sms.emse.fr (M.J. Jones).

1359-6454/03/$30.00
doi:10.1016/S1359-6454(03)00002-8

of the precipitation, and the presence of precipitates may interfere with the recovery and recrystallization processes. Although the interaction of precipitation and recrystallization was investigated around 25 years ago by Hornbogen and colleagues [e.g. 1, 2], little recent work has been reported in this area, and many aspects of the physical processes involved remain unclear.

There is currently considerable interest in the potential use of the coherent Al_3Sc trialuminide phase in aluminium-based aerospace and automotive alloys [e.g. 3]. This is due to its exceptional thermal stability and high number density, which has been found to both severely inhibit the onset of recrystallization and impart a significant strengthening effect in aluminium [4,5]. Whilst the nucleation and precipitation kinetics of the Al_3Sc phase in undeformed aluminium have been well documented in recent years [e.g. 6], many aspects of the underlying recrystallization-precipitation interaction mechanisms and subsequent microstructural evolution in deformed and annealed Al-Sc alloys, are far from clear.

The purpose of the present work is to investigate the interaction between recrystallization and precipitation in three deformed and annealed binary Al-Sc alloys (Al-0.02, 0.12 and 0.25wt.%Sc). Particular emphasis was placed on the use of electron backscatter diffraction (EBSD) and transmission electron microscopy (TEM) in order to study the evolution of microstructure, microtexture and the interaction of boundaries with particles.

2. Materials and experimental methods

Three high purity binary Al-Sc alloys of composition Al-0.02, 0.12 and 0.25wt.%Sc were supplied by Alcan International Ltd, Banbury Laboratory, in the form of 25 mm DC cast bookmoulds (alloy variants will subsequently be referred to as either 0.02, 0.12 or 0.25%Sc). The solubility of scandium in aluminium is ~0.02 at ~300 °C, and the alloy of this composition can be taken to represent the single-phase matrix material of all the alloys. All alloys were initially solution heat-treated above the solvus in an air furnace for 72 h, and water-quenched to ambient temperature. The grain size after solution treatment was very large, typically ~1 mm. The solution treatment temperatures and the initial grain sizes of the materials are given in Table 1. Additionally, a small number of solution treated 0.12%Sc and 0.25%Sc samples were pre-aged at 400 °C in an air furnace for 16 h and water-quenched prior to testing. Samples were then deformed by cold rolling to 80% reduction. Deformed specimens were sectioned in the plane parallel to the normal direction (ND) and rolling direction (RD), and annealed either in a salt bath (heating rate ~500 °C/s) or in an air furnace programmed to give a heating rate of 10 °C/h. All samples were water quenched after annealing.

In order to follow the microstructural evolution during annealing, specimens were mechanically polished, anodized in Barkers reagent, and examined under polarised light to reveal differing crystallographic orientations. Specimens for scanning electron microscopy (SEM) and EBSD were mechanically polished, followed by an electropolish in 70:30 methanol/nitric acid solution at −30 °C. Specimens were examined with backscattered electrons using both a Phillips XL-30 FEG-SEM and a CAMSCAN 2040SA FEG-SEM operated at 8–10 kV. Spatial orientations of selected regions and orientation maps were obtained from electropolished SEM specimens using the HKL Channel EBSD acquisition system. Data analysis was performed using VMAP software developed in-house [7]. In the EBSD maps presented in this paper, high-angle grain boundaries (HAGBs), of misorientation $>15°$, are shown as solid black lines and low angle grain boundaries (LAGBs), of misorientation $>1.5°$, are shown as solid white lines. All optical and SEM/EBSD micrographs were taken in the ND-RD plane and are presented such that the RD is horizontal, and the ND is vertical.

Table 1
Homogenisation treatments and initial grain sizes

Alloy	Homogenisation/solution treatment	Initial grain size/mm
0.02%Sc	500 °C	0.2–1
0.12%Sc	600 °C	0.1–1
0.25%Sc	640 °C	0.5–5

Thin foils for transmission electron microscopy (TEM) studies were prepared by electropolishing discs of 3 mm diameter, spark eroded from sections of the same plane and were examined using a Phillips EM400T, a Phillips CM200 and a Phillips EM430ST at 120, 200 and 300 kV respectively.

Because of the very large initial grain sizes, there was substantial variation in the deformation and annealing microstructures and the textures throughout the samples. This made quantitative evaluation of the mean microstructural parameters unreliable, and consequently few quantitative analyses of microstructure and texture are presented in this paper.

3. Results and discussion

3.1. The deformed state

The alloys were deformed in the solution treated single-phase condition (or with fine Al_3Sc particles present in the case of pre-aged alloys). Alloys examined in the as-deformed state at optical level, revealed microstructures where the very large prior grain size gave large grain to grain and sample to sample variability in terms of any grain subdivision. Coarse scale deformation banding was seen within some grains, although other grains appeared to have deformed more homogeneously (see Fig. 5). More detailed microstructural examination revealed well-defined cellular structures bounded by diffuse arrays of dislocations. The cells, which were found to contain low levels of interior dislocations, had a mean size of ~0.5 μm, and misorientations of 1~2°.

These microstructures were typical of deformed large-grained single-phase dilute aluminium alloys, and were very similar to those found in similarly large-grained deformed Al-Mn alloys [8].

3.2. Precipitation in Al-Sc alloys

The aluminium-rich end of the Al-Sc phase diagram has a eutectic point at 655 °C & 0.5wt.%Sc, and the maximum solid solubility of Sc is 0.35wt.% at this temperature. However, the solid solubility decreases markedly at lower temperatures and at 500 °C the solubility is less than 0.1%. Precipitation of coherent Al_3Sc ($L1_2$ structure) from supersaturated solid solution has been found to occur by homogeneous nucleation and growth [e.g. 4]. The critical Al_3Sc nucleus radius has been found to be 4.07 Å [9], which is very close to the Al_3Sc unit cell dimension (i.e. 4.105 Å), and which results in a small nucleation barrier for precipitation and a high rate of decomposition, even in the absence of a dislocation structure.

At low annealing temperatures, the particles in the 0.25%Sc alloy were found to be approximately spherical and coherent with the matrix (see Fig. 1), and coherency was lost between 450 and 500 °C when the particle size was ~20 nm. Larger particles were semi-coherent (see Fig. 1), and although they remained equiaxed, some faceting of the interfaces was observed. These observations are consistent with previous work on alloys of compositions between 0.2 and 0.3wt.%Sc [4,6]. The experimentally measured particle sizes in samples of 0.25%Sc, aged for 1 h at various temperatures, are plotted in Fig. 1 for temperatures in the range 400–600 °C.

The particle growth in the 0.25%Sc alloy was found to obey a relationship of the form

$$\bar{r} = A\sqrt{\exp\left(\frac{-Q}{RT}\right)}\cdot t \qquad (1)$$

where the constant A which contains the pre-exponential factor and supersaturation function, is

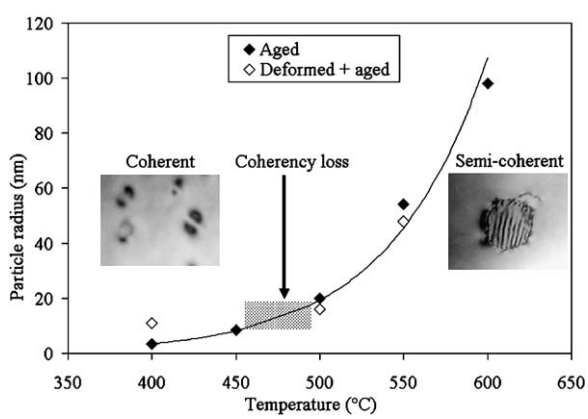

Fig. 1. Precipitate growth in Al-0.25wt.%Sc during a 1 h anneal.

~$1.20.10^{-4}$ and Q, the activation energy for precipitation is ~163 $kJmol^{-1}$, and the curve from Eq. (1) is fitted to the experimental data in Fig. 1. These kinetics and the activation energy for precipitate growth are quite similar to those of a previous investigation of precipitation in Al-0.3wt.%Sc [6]. It should be noted that there is no discontinuity in the coarsening curve when coherency is lost, and this is consistent with the rate of coarsening being controlled by bulk diffusion.

Also shown in Fig. 1 are experimental points obtained in the present study from material which had been deformed in the solution treated condition before aging. The experimental evidence presented in Fig. 1 shows that the kinetics of precipitate growth are similar in the presence of a (recovered) deformation structure to those of the undeformed and aged material. The lack of any significant effect of a deformed microstructure on the precipitation or coarsening kinetics is not surprising in an alloy system where the precipitation is occurring homogeneously.

The precipitation in the 0.12%Sc alloy is rather different from that of the 0.25%Sc alloy discussed above. In the 0.12%Sc alloy, precipitation appears to be heterogeneous (at least in the temperature range 400–450 °C), where large irregularly shaped particles of size 100–200 nm are formed at dislocations and boundaries. It is well known that a large driving force is required for homogeneous precipitation, and it is therefore not surprising that for the more dilute alloy there is insufficient driving force for homogeneous precipitation, particularly at the high aging temperatures employed in the present investigation, and that the precipitation is therefore heterogeneous. This behaviour is similar to that found by Marquis and Seidman [6] in an Al-0.1wt.%Sc alloy, to which the reader is referred for further details. The precipitation behaviour of the 0.12%Sc alloy is rather similar to that found in a deformed and annealed Al-1.3wt.%Mn solid solution [10], where it was found that precipitation occurred inhomogeneously at both LAGBs and HAGBs and was therefore strongly affected by the presence of a deformation substructure.

3.3. Recrystallization kinetics

The recrystallization kinetics of the three alloys which had been cold rolled 80% in the solution treated condition, and annealed in a salt bath, were measured using optical microscopy. Fig. 2 shows the start (~5%) and finish (~95%) of recrystallization for each material. The 0.02%Sc alloy recrystallizes in the temperature range 250–300 °C, which is typical of a low solute single-phase aluminium alloy [e.g. 1], and there is no evidence of any precipitation in this material. The behaviour of this alloy, can be used as a guideline for interpreting the recrystallization behaviour of the other alloys.

The 0.25%Sc alloy, commences recrystallization at ~500 °C. This behaviour is consistent with precipitation being complete before recrystallization starts. The second-phase particles prevent recrystallization until particle coarsening reduces the pinning of low angle and high angle boundaries until the pinning pressure (P_Z) is less than the driving pressure (P_D) for recrystallization. Although, as discussed above, quantitative analysis in such an inhomogeneous microstructure is difficult, the recrystallization behaviour can be shown to be consistent with the precipitation. The analyses below take the particle sizes obtained after a 1 h anneal as given by Fig. 1.

The driving pressure for recrystallization, P_D for a recovered microstructure of subgrains (diameter D) and boundary energy γ_S can be taken [1] as

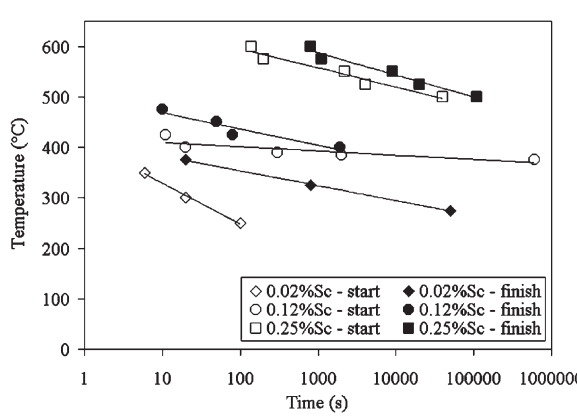

Fig. 2. Isothermal recrystallization kinetics for the Al-Sc alloys.

$3\gamma_S/D$. D ~1μm, and γ_S for 1° boundaries is estimated from the Read-Shockley equation to be ~0.2 of the energy (γ_H) of a high angle boundary (0.32 Jm^{-2} [11]), and thus P_D ~0.4 MPa.

The Zener pinning pressure for a volume fraction F_V of coherent particles of diameter d is $6F_V\gamma_H/d$ [see e.g. 1]. At 450 °C, d ~ 17 nm and $F_V \sim 7 \times 10^{-3}$, giving P_Z ~0.8 MPa. As $P_Z > P_D$, recrystallization is inhibited at this temperature. However, at 550 °C, d ~ 108 nm and $F_V \sim 5 \times 10^{-3}$ and thus P_Z ~ 0.1 MPa, and as $P_Z < P_D$, it is now possible for recrystallization to proceed.

In the 0.12%Sc alloy, recrystallization commences at a temperature of ~375 °C. However, it is clear from the almost horizontal recrystallization start line in Fig. 2, that at this temperature recrystallization does not proceed to any great extent, and that complete recrystallization does not occur within the times investigated until temperatures of 400 °C and above. This indicates that in this temperature range, precipitation starts before recrystallization is complete, leading to a complex interaction between the processes of precipitation and recrystallization, which is discussed in detail in section 3.4.2. Precipitation in the undeformed 0.12%Sc alloy occurs on defects and is coarse and slow, whereas the recrystallization kinetics of Fig. 2 suggest that the presence of the deformed structure has enabled the rapid fine-scale precipitation on boundaries, which is necessary to hinder or prevent recrystallization, in a similar manner to that found in Al-Mn alloys [10]. Backscattered electron imaging in the SEM confirmed that fine-scale heterogeneous precipitation was indeed occurring, as shown in Fig. 3. This micrograph, in which the Al_3Sc particles appear white, shows a recrystallization front in a deformed sample annealed for 5 min at 380 °C.

In the recrystallized grain (A), some small (20–30 nm) irregularly spaced particles are seen. These probably precipitated on the deformed substructure before recrystallization, and have not grown significantly since. At the high angle boundary (B) defining the recrystallization front, and in the recovered region (C), much larger (50–100 nm) particles are seen to pin the high and low angle boundaries. The continued presence of substructure for the whole of the anneal has enabled these particles

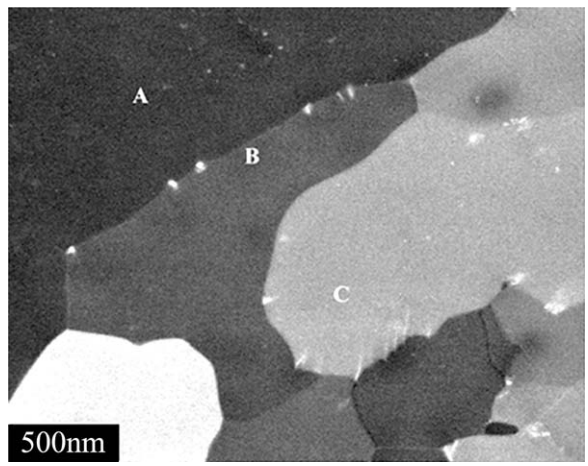

Fig. 3. Backscattered electron SEM micrograph showing heterogeneous precipitation in 0.12wt.%Sc annealed 5 m at 380 °C.

to grow more than those in the recrystallized grain (A).

Although, because of the short annealing times and irregular nature of the precipitation, detailed kinetics of the precipitation in the deformed and annealed 0.12%Sc alloy have not been obtained, the semi-quantitative diagram of Fig. 4 shows the proposed relationship between precipitation and

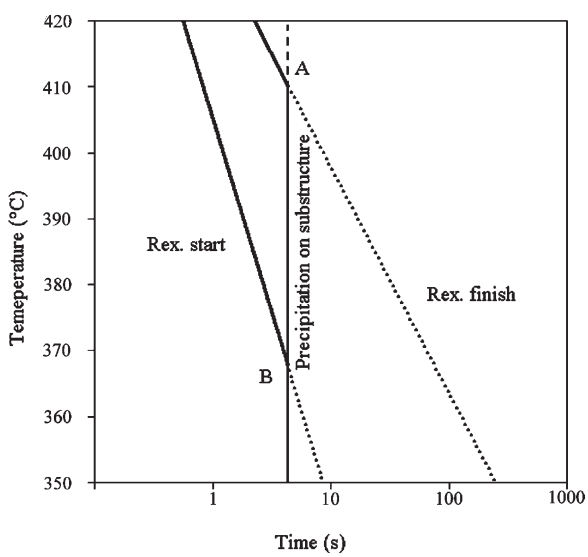

Fig. 4. Semi-quantitative representation of the interaction between precipitation and recrystallization in Al-0.12wt.%Sc.

recrystallization in this material during isothermal annealing. The recrystallization start and finish lines are based on the data for the single-phase 0.02%Sc alloy. The bold lines indicate the processes which occur in the 0.12%Sc alloy, whilst the dotted lines indicate those which do not occur in this alloy. The "precipitation" line, which is mainly based on microstructural observations and on the recrystallization kinetics of the 0.12%Sc alloy shown in Fig. 2, indicates the time at which sufficient precipitation has occurred on the deformation substructure to hinder or prevent recrystallization. The difference in the temperature sensitivities of recrystallization and precipitation is due to two factors. At lower temperatures precipitation becomes more rapid than recrystallization due to the increased driving pressure from the increased supersaturation. Additionally, although both recrystallization and precipitation are dominated by volume diffusion, the growth of heterogeneous precipitates on boundaries will involve some boundary diffusion which has a lower activation energy. There are three significant temperature regimes shown in Fig. 4 [cf 2]:

1. At annealing temperatures below B (~370 °C), recrystallization is prevented by prior precipitation on the substructure.
2. At annealing temperatures above A (~410 °C), recrystallization is finished before significant precipitation occurs.
3. At intermediate temperatures, some recrystallization occurs, e.g. in those parts of the microstructure with highest stored energy, but subsequent precipitation on the substructure prevents its completion. The fraction of recrystallization is only weakly dependent on time, but increases as the temperature is raised from ~370–410 °C, as recrystallization commences earlier.

3.3.1. The effect of pre-aging on recrystallization

The results discussed above were obtained by annealing solution treated and deformed material. The effects of aging the 0.25%Sc and 0.12%Sc alloys prior to deformation were also investigated by annealing the solution treated alloys for 16 h at 400 °C before deformation. It was found that the 0.25%Sc material was fully recrystallized after annealing for 1 h at 575 °C (Table 2), and comparison with Fig. 2 or the "normal schedule" (annealing of solution treated and deformed samples in a salt bath) in Table 2, shows that the pre-aging has had no significant effect. This is because deformation has little influence on the precipitation kinetics in this alloy (Fig. 1) and precipitation is always more rapid than recrystallization. Thus recrystallization is delayed until sufficient particle coarsening has occurred ($P_D > P_Z$).

It was found that the pre-aged 0.12%Sc alloy did not commence recrystallization until 1 h at 500 °C, whereas reference to Fig. 2 shows that the non-aged material started to recrystallize below 400 °C. As precipitation in this alloy within this temperature range is known to be coarse and heterogeneous in undeformed material (section 3.2), it is difficult to understand why a pre-aging treatment should have any significant effect. One possible explanation is that the pre-aging produces some solute clustering which accelerates precipitation after deformation and annealing, compared with the non-aged material. Because recrystallization and precipitation are occurring simultaneously in this material as discussed above and shown in Fig. 4, any slight acceleration of the precipitation will lead to significantly retarded recrystallization.

3.3.2. The effect of heating rate on recrystallization

The results discussed above were obtained by annealing in a salt bath with a heating rate of ~500 °C/s. As it is known that heating rate can have a significant effect on the recrystallization kinetics in some two-phase alloys, the effects of heating rate were investigated by heating solution treated and deformed samples to temperature at 10 °C/h and holding for 1 h.

Table 2
Temperatures at which recrystallization is complete after 1 h

Alloy	Normal schedule	Pre-age	Slow heat
0.12%Sc	400 °C ± 10	> 500 °C	500 °C ± 10
0.25%Sc	575 °C ± 10	575 °C ± 10	550 °C ± 10

The results summarised in Table 2 show that the recrystallization behaviour of the 0.25%Sc alloy was little affected by the heating rate, because the precipitation always occurred before the start of recrystallization. However, the recrystallization of the 0.12%Sc alloy was significantly retarded at the slow heating rate. This result is similar to that found in other alloys in which precipitation and recrystallization compete, [1,10,12,13] and is thought to be due to small changes in the relative rates of the competing processes of precipitation and recrystallization. Even if both processes have similar activation energies, precipitation will be accelerated relative to recrystallization at low temperatures due to the increased driving force arising from the larger supersaturation (Fig. 4), and therefore slow heating will allow more precipitation to occur before recrystallization than will rapid heating.

3.4. Microstructural evolution during annealing

3.4.1. Recrystallization of Al-0.25wt.%Sc

As these are high purity alloys with no large second-phase particles present, the sites for recrystallization are either pre-existing high angle grain boundaries, or high angle boundaries generated during deformation, and at a sufficiently high temperature, recrystallization originates at these sites as shown in Fig. 5. This micrograph illustrates the heterogeneity typical of these large-grained samples. The upper part of the micrograph shows a grain which has fragmented extensively, whilst the lower grain is homogeneous on the optical scale. A portion of the boundary between the two grains has grown into the lower grain, probably by a process of strain induced boundary migration (SIBM) [1].

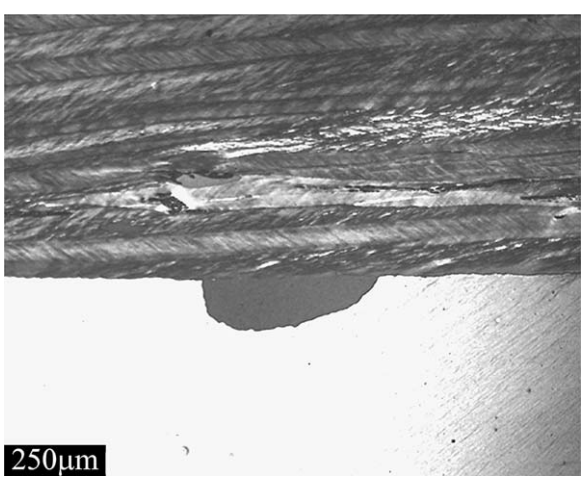

Fig. 5. Optical micrograph of partially recrystallized 0.25wt.%Sc, annealed in a salt bath for 1 m at 575 °C.

The driving pressure for the recrystallization (P_D) is provided by the stored energy of deformation, and simple models [1,14] predict that a portion of boundary of length L and specific energy γ can migrate by SIBM if

$$L \geq \frac{2\gamma}{P_D} \tag{2}$$

However, the precipitation which precedes recrystallization as discussed above, produces a boundary pinning pressure (P_Z), and thus Eq. (2) becomes

$$L \geq \frac{2\gamma}{(P_D - P_Z)} \tag{3}$$

Clearly no recrystallization can occur when $P_Z > P_D$, but as the precipitate coarsens and P_Z is reduced, SIBM involving long boundary segments (L), such as the 300 μm segment seen in Fig. 5 can occur. In a situation where P_Z falls during annealing, thereby reducing the critical value of L, a few suitable large boundary segments will recrystallize first and dominate the microstructure, resulting in a very large grain size, and Fig. 6 shows the 0.25%Sc alloy almost recrystallized, with a grain size of ~1 mm. The grains are elongated in the rolling direction, and this is probably due to the additional pinning produced by precipitates at the existing grain boundaries, which make it difficult for a recrystallizing grain to migrate easily in the normal direction [15].

3.4.2. Recrystallization of Al-0.12wt.%Sc

In contrast to the 0.25%Sc alloy, recrystallization in the 0.12%Sc alloy was affected but not completely inhibited by precipitation. Fig. 2 shows that a small amount of recrystallization occurred on annealing at 375 °C for a short period, but that little further recrystallization occurred on holding at this temperature, and that full recrystallization only occurred at temperatures of 400 °C and above.

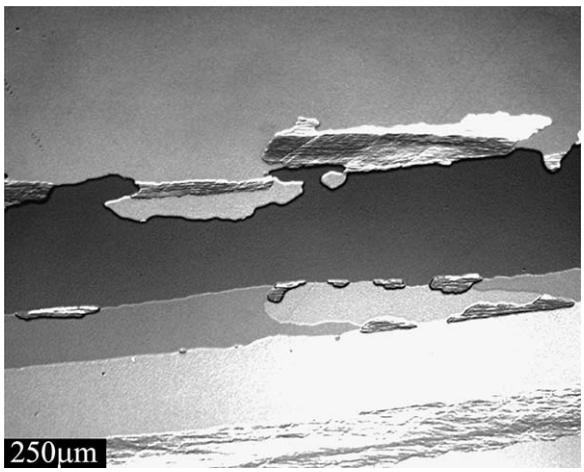

Fig. 6. Optical micrograph of partially recrystallized 0.25wt.%Sc, annealed in a salt bath for 4.5 h at 525 °C.

At temperatures in the range 375–450 °C, the recrystallizing or recrystallized microstructures were found to be very heterogeneous, as shown in Fig. 7(a), making them difficult to quantify. Even in single-phase aluminium alloys, it is well established that grains of different orientation have different stored energies and will recrystallize at different rates to different grain sizes [see e.g. 1]. However, the differences in recrystallization behaviour between grains such as is seen in Fig. 7(a), is more pronounced in alloys in which precipitation is occurring during recrystallization [10]. This is interpreted in terms of the relative rates of precipitation and recrystallization in different grains being affected by differences in the deformation substructure of the grains. At higher annealing temperatures more equiaxed microstructures evolved as shown in Fig. 7(b), and this is consistent with recrystallization being completed before the occurrence of significant precipitation. Recrystallization in the temperature range 375–450 °C was characterised by two particular features of interest.

3.4.3. Broad front SIBM

Recrystallization was found to originate at pre-existing high angle boundaries by strain-induced boundary migration (SIBM), and it was often found that very large lengths of boundary (up to ~1 mm) migrated by this mechanism as shown in

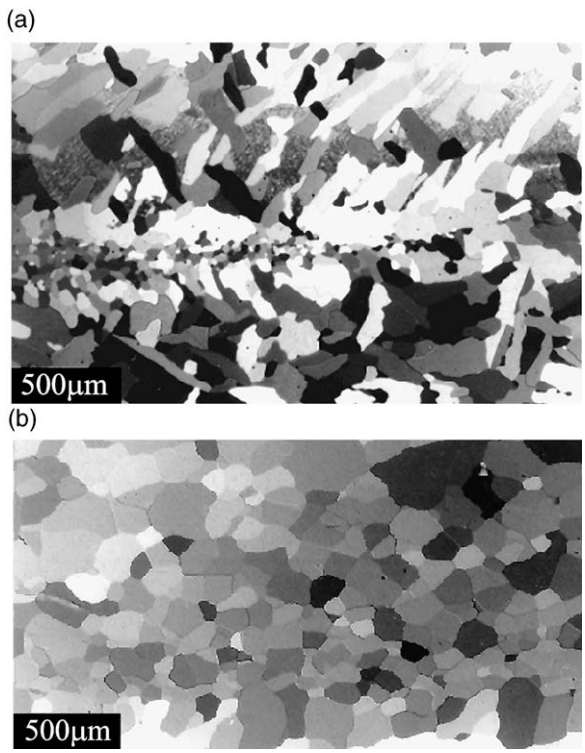

Fig. 7. (a) Optical micrograph of partially recrystallized 0.12wt.%Sc, annealed in a salt bath for 5 m at 400 °C. (b) Optical micrograph of recrystallized 0.12wt.%Sc, annealed in a salt bath for 1 m at 475 °C.

the example of Fig. 8. In this EBSD map, a cube-oriented grain at the bottom is growing into Goss-oriented deformed material, with low or medium angle boundaries (~10°) being dragged behind the migrating HAGB. Such broad front SIBM is not typical of single-phase alloys, but has been reported in particle-containing aluminium alloys

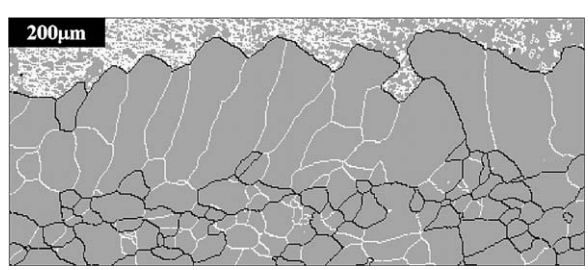

Fig. 8. EBSD map showing broad front SIBM in an Al-0.12wt.%Sc sample annealed 20 s at 425 °C. The HAGB's are shown as black and LAGB's as white.

[10,16], and is explained by the large critical boundary length (L) required for SIBM in alloys with a dispersion of pinning particles (Eq. (3)). The difference between SIBM in the 0.25%Sc and 0.12%Sc alloys is that in the former, SIBM is delayed until particle coarsening or dissolution has unpinned the boundary segments. In the 0.12%Sc alloy, as in Al-Mn [10], precipitation is heterogeneous and irregular. Some boundaries will be pinned before SIBM can occur and others will undergo SIBM before pinning by precipitation occurs.

3.4.4. Faceted boundaries

As seen in the partly recrystallized sample of Fig. 9, many of the recrystallizing grains were distinctly faceted. EBSD analysis showed that many of the faceted grains were growing into relatively homogeneously deformed grains, and had orientation relationships of 25–35° about axes within ~10° of either <111> or <112>. Traces of the facets were found to be consistent with the recrystallizing grains having a faceted tilt boundary and one or more faceted twist boundaries. This type of faceting is not normally found for recrystallizing grains in single-phase aluminium alloys and is thought to be a consequence of precipitation occurring simultaneously with recrystallization. Although the origins of this effect require further clarification, the faceting may be due to lower Zener drag on certain special boundaries as has been found for copper [17] or to a dependence of precipitation kinetics on boundary character [10,18].

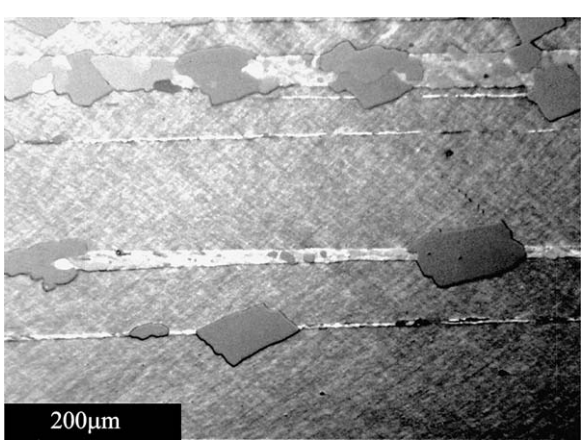

Fig. 9. Optical micrograph showing faceted recrystallizing grains in 0.12wt.%Sc, annealed in a salt bath for 20 s at 425 °C.

3.5. Grain boundary-precipitate interactions in Al-0.25wt.%Sc

When the deformed 0.25%Sc solid solution is annealed, the particles are initially fully coherent with the matrix. There is evidence from the literature that the interaction of migrating boundaries with coherent particles may lead to several effects including loss of coherency or dissolution and re-precipitation [1], and it was therefore of interest to investigate the effects of the annealing processes on the particles.

It was shown in section 3.2 that the precipitates lost full coherency at a radius greater than ~20 nm. On annealing the deformed 0.25%Sc alloy at temperatures below ~550 °C, the small (<20 nm) coherent precipitates were very effective at pinning LAGBs and preventing recrystallization. However at higher temperatures (e.g. 575 °C) it was found that some local LAGB migration occurred and there was evidence that as a LAGB passed a precipitate, the particle both grew (e.g. from a radius of ~15–24 nm) and became semi-coherent. This is shown in Fig. 10, where smaller coherent particles are seen at the top of the micrograph above the LAGB. At the bottom of the micrograph a larger semi-coherent particle with moiré fringes is seen, and in the boundary, particles are seen transforming from coherent to semi-coherent. It is likely that pipe diffusion in the low angle boundary enhances the coarsening kinetics of a precipitate located on the boundary. The coarsened semi-coherent particles will exert a lower pinning pressure on the boundary, and this will eventually allow the boundary to migrate.

During recrystallization of the 0.25%Sc alloy, the high angle grain boundaries were found to pass through the semi-coherent particles as shown in Fig. 11, and this was confirmed by dark field imaging using particle reflections. Thus the particles remained semi-coherent even after recrystallization, having undergone the same orientation change as the grain surrounding it. A similar effect has previously been observed for coherent γ' particles in nickel alloys [19], and this process is

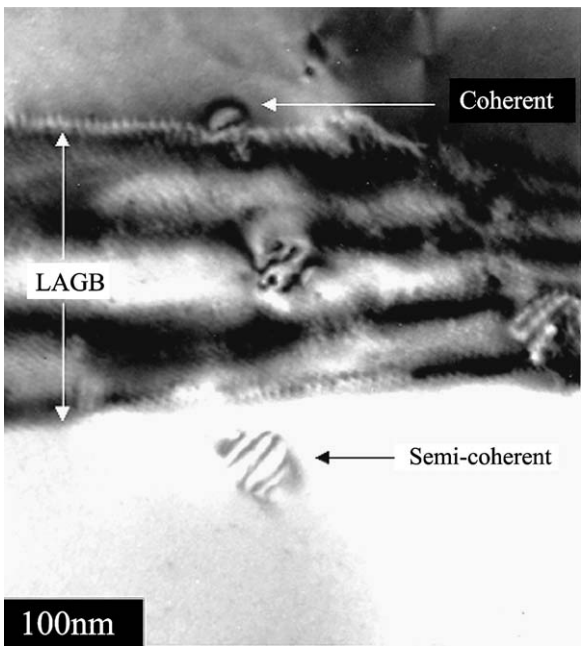

Fig. 10. Transmission electron micrograph showing change from coherency to semi-coherency during the passage of a low angle boundary in Al-0.25wt.%Sc annealed 1 m at 575 °C.

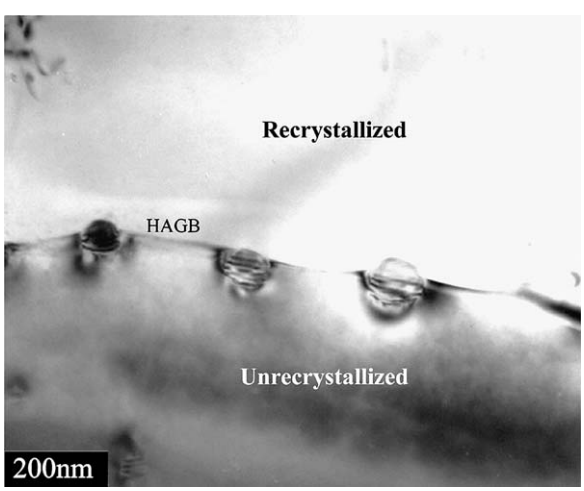

Fig. 11. Transmission electron micrograph showing migration of a high angle boundary through a dispersion of semi-coherent particles in Al-0.25wt.%Sc annealed 5 m at 575 °C.

rather different to the particle dissolution and renucleation of coherent particles proposed by Doherty [20].

4. Conclusions

1. The precipitation and growth kinetics of Al_3Sc particles in an Al-0.25wt.%Sc alloy are found to be unaffected by the presence of a deformation substructure. However, precipitation in an Al-0.12wt.%Sc alloy is heterogeneous, and is greatly accelerated by the presence of a deformation structure.
2. In deformed supersaturated Al-0.25wt.%Sc solid solutions, precipitation occurs before recrystallization, and recrystallization only occurs at long times or very high temperatures (>500 °C), when the particle pinning pressure is sufficiently reduced.
3. In deformed supersaturated Al-0.12wt.%Sc solid solutions, recrystallization is severely impeded below ~370 °C, due to precipitation starting before recrystallization. Above this temperature recrystallization and precipitation occur simultaneously, resulting in irregular microstructures containing a number of unusual features such as faceted boundaries and broad front SIBM. At temperatures above ~400 °C, recrystallization precedes precipitation, resulting in microstructures typical of a single-phase aluminium alloy.
4. Coherent precipitates in Al-0.25wt.%Sc are found to coarsen and become semi-coherent during the passage of low-angle boundaries during recovery.
5. The passage of high-angle boundaries through semi-coherent precipitates during recrystallization of Al-0.25wt.%Sc occurs by migration of the boundary through the particle, resulting in the precipitates maintaining semi-coherency with the new grains.

Acknowledgements

The authors would like to acknowledge the financial support of both the Engineering and Physi-

cal Sciences Research Council and Alcan International Ltd. (who provided the materials). We also thank Mr Ian Brough and Mr Peter Kenway of The Manchester Materials Science Centre for assistance with EBSD and TEM work respectively.

References

[1] Humphreys FJ, Hatherly M. In: Recrystallization and related annealing phenomena, 1st edn. Pergamon; 1995.
[2] Hornbogen E, Köster U. In: Haessner F, editor. Recrystallization of metallic materials. Stuttgart, Germany; 1978.
[3] Harada Y, Dunand DC. Acta Mater 2000;48:3477.
[4] Røyset J, Ryum N. In: Sanders T. et al., editor. Proc 4th Int Conf on Aluminium Alloys I. Atlanta, USA: Georgia Inst. Tech.;1994. p. 194.
[5] Miura Y, Shioyama T, Hara D. In: Driver JH. et al., editor. Proc 5th Int Conf on Aluminium II. Grenoble, France: Trans Tech. Pub.;1996. p. 505.
[6] Marquis EA, Seidman DN. Acta Mater 2001;49:1909.
[7] Humphreys FJ. J. Mat. Sci. 2001;36:3833.
[8] Somerday M, Humphreys FJ. Mats Sci and Tech 2002 (in press)—part 2.
[9] Hyland Jr. RW, Asta M, Foiles SM, Rohrer CL. Acta Mater 1998;46:3667.
[10] Somerday M, Humphreys FJ. Mats Sci and Tech 2002 (in press)—part 1.
[11] Murr LE. Interfacial phenomena in metals and alloys. Reading: Addison-Wesley, 1975.
[12] Bowen AW. Mats Sci and Tech 1990;6:1058.
[13] Wert JA, Paton NE, Hamilton CH, Mahoney MW. Metall Trans 1981;12A:1267.
[14] Bailey JE, Hirsch PB. Proc R Soc Lond 1962;A267:11.
[15] Nes E, Ryum N, Hunderi O. Acta Metall 1985;33:11.
[16] Higginson R, Bate P. Acta Mater 1999;47:1079.
[17] Humphreys FJ, Ardakani MG. Acta Mater 1996;44:2717.
[18] Daaland O, Nes E. Acta Mater 1996;44:1413.
[19] Randle V, Ralph B. Acta Metall 1986;34:891–8.
[20] Doherty RD. Metal Sci 1982;16:1.